Eruptions that Drive Coronal Jets in a Solar Active Region

Alphonse C. Sterling[1], Ronald L. Moore[1,2], David A. Falconer[1,2], Navdeep K. Panesar[1,2], Sachiko Akiyama[3,4], Seiji Yashiro[3,4], & Nat Gopalswamy[3]

[1]Heliophysics and Planetary Science Office, ZP13, Marshall Space Flight Center, Huntsville, AL

[2]Center for Space Plasma and Aeronomic Research (CSPAR), UAH, Huntsville, AL

[3]NASA Goddard Space Flight Center, Greenbelt, MD 20771, USA

[4]The Catholic University of America, Washington, DC 20064, USA

Abstract

Solar coronal jets are common in both coronal holes and in active regions (e.g., Shibata et al. 1992, Shimojo et al. 1996, Cirtain et al. 2007. Savcheva et al. 2007). Recently, Sterling et al. (2015), using data from Hinode/XRT and SDO/AIA, found that coronal jets originating in polar coronal holes result from the eruption of small-scale filaments (minifilaments). The jet bright point (JBP) seen in X-rays and hotter EUV channels off to one side of the base of the jet's spire develops at the location where the minifilament erupts, consistent with the JBPs being miniature versions of typical solar flares that occur in the wake of large-scale filament eruptions. Here we consider whether active region coronal jets also result from the same minifilament-eruption mechanism, or whether they instead result from a different mechanism (e.g. Yokoyama & Shibata 1995). We present observations of an on-disk active region (NOAA AR 11513) that produced numerous jets on 2012 June 30, using data from SDO/AIA and HMI, and from GOES/SXI. We find that several of these active region jets also originate with eruptions of miniature filaments (size scale ~20'') emanating from small-scale magnetic neutral lines of the region. This demonstrates that active region coronal jets are indeed frequently driven by minifilament eruptions. Other jets from the active region were also consistent with their drivers being minifilament eruptions, but we could not confirm this because the onsets of those jets were hidden from our view. This work was supported by funding from NASA/LWS, NASA/HGI, and Hinode. A full report of this study appears in Sterling et al. (2016).

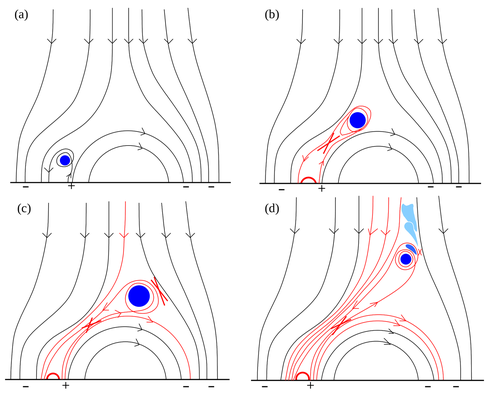

Fig. 1. Schematic showing in 2D the formation process of jets, as suggested by Sterling et al. (2015). The dark blue feature is cool minifilament material, enveloped by sheared magnetic field. Red/black lines show field that has/has not undergone magnetic reconnections, and "X"-es show reconnection locations. The bold red semicircle in (b)---(d) show the jet bright point (JBP), formed by internal reconnection beneath the erupting minifilament. (Such JBPs are common features of observed jets, appearing off to one side of the base of jet spires.) In (c) external (aka interchange) reconnection has made a new open field line, where the hot (X-ray and hot EUV) jet forms. In (d) the external reconnection has eaten through the outer minifilament field so that the cool material enters the open field, forming a cool (e.g., 304 Å) jet.

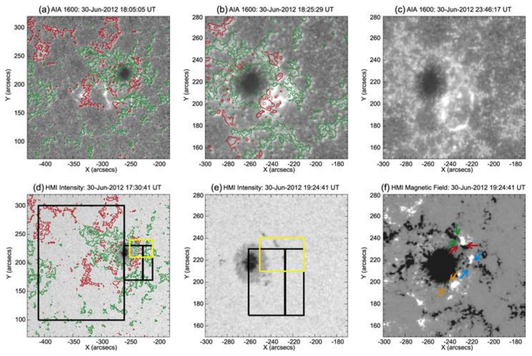

Fig. 2. Active region of this study at indicated wavelengths. Panels (a)-(c) are at times of Table 1 events 3, 4, and 10, respectively. Boxes in (d) and (e) are labeled in Fig. 3(d). Arrow pairs in (f) are neutral lines on which jets occur. Overlaid onto panels (a), (b), and (d) are HMI magnetograms, where red and green respectively represent positive and negative polarities, and where the contours are at levels of ±50, ±100, and ±750 G, and where the magnetograms in (a), (b), and (d) are respectively at 18:06 UT, 18:25 UT, and 17:30 UT on 2012 June 30.

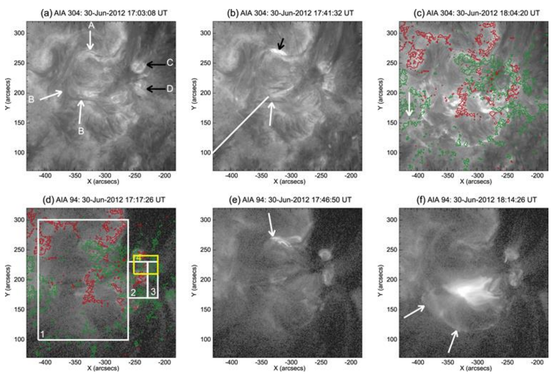

Fig. 3. Active region around time of Table 1 event 3. This was an eruption of a large-scale filament (B arrows). It appears to be a scaled-up version of the erupting jets (compare circular illuminations in 3f of the large-scale filament eruption, with that in Fig. 2c from a jet/spray eruption.) Boxes in (d) show regions where intensity curves were calculated (e.g. in Figs. 6 and 8).

References:
Cirtain, Golub, Winebarger, et al. 2007, Science, 318, 1580
Savcheva, Cirtain, DeLuca, et al. 2007, PASJ, 59S, 771S
Shibata, Ishido, Acton, et al. 1992, PASJ, 44L, 173
Shimojo, Hashimoto, Shibata, Hirayama, Hudson, & Acton 1996, PASJ, 48, 123
Sterling, Moore, Falconer, & Adams 2015, Nature, 523, 437
Sterling, Moore, Falconer, et al. 2016, ApJ, 821, 100
Yokoyama & Shibata 1995, Nature, 375, 42

Table 1
GOES List for Events of Figure 4, and CME Properties

Jet/Event	Time (UT)[a]	Flare	Region[b]	CME?[c]	CME Time (UT)[c]	Width (deg)[c]	Velocity (km s^{-1})[c]
1	17:28	B6.0	C	Probably	17:35	4.0 ± 0.6	458 ± 66
2	17:47	B7.0	A	No	…	…	…
3	18:12	C1.6	B	Yes	18:10	62.8 ± 1.4	300 ± 9
4	18:33	M1.6	D	Probably	18:40	26.7 ± 3.6	482 ± 102
5	19:32	B7.0	C	Yes	19:40	7.7 ± 1.6	368 ± 44
6	20:19	B8.0	C	Probably	20:20	4.3 ± 0.6	479 ± 17
7	20:28	B9.0	A	Probably	20:35	3.3 ± 0.6	521 ± 32
8	21:26	C1.6	C	Yes	21:30	7.2 ± 2.5	841 ± 10
9	22:37	C1.1[d]	C	Maybe	22:45	2.6 ± 0.9	356 ± 61
10	23:54	C1.0	D	Maybe	23:50	8.0 ± 2.8	515 ± 39
11	00:09	B6.0	A and C	No	…	…	…

Notes.
[a] Time of peak brightening (within ≲1 minute) in *GOES* 1–8 Å X-ray flux on 2012 June 30 (July 1 for event 11); event 3 is a filament eruption, while other events are jets. In some cases the CME appears prior to the peak in X-ray flux, but this is consistent with other observations (e.g., Harrison 1986).
[b] Region in Figure 3(a) where the source of the event is located.
[c] Indicates whether a CME was detected from the event in *STEREO-B*/Cor1 images. If not "no," then entries in column 5 reflect the level of confidence that the observed CME originates from the event. Subsequent columns give the time of the CME's first appearance in *STEREO-B* Cor1 images, and the angular width and plane-of-sky velocity of the CME. Widths and velocities are averages of four measurements, and uncertainties are 1σ standard deviations.
[d] Much or most of this emission is from a different active region, AR 11514 (S17E18).

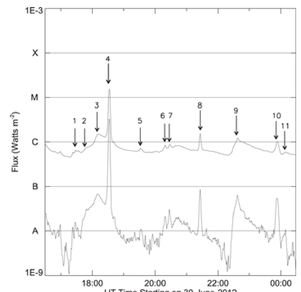

Fig. 4. Soft X-ray (SXR) fluxes from GOES 1—8 Å (top) and 0.5—4 Å (bottom) channels. Arrows show events identified from AIA 94 Å movies over the FOV of Fig 3. Table 1 gives details of the arrowed events.

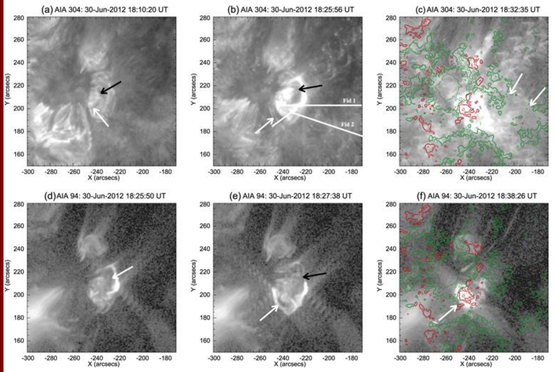

Fig. 5. Images showing jet of Table 1 event 4 at indicated wavelengths. In (a), the white/black arrows show two minifilament segments that erupted at the start of the jet. In (b), those two segments have merged into a single erupting minifilament ("precursor minifilament") (black arrow), and a third minifilament segment (white arrow) has just started rising upward; we call this third segment the "main minifilament" of this jet, since it erupts most violently. Fiducial 1 in (b) shows the path over which we measure the trajectory of the precursor minifilament. Fiducial 2, with the bend in it, is for the main minifilament. Arrows in (c) show the outward-expelled jet. Arrows in (d) and (e) also point to the minifilament segments. In (f) the bright emission (arrow) is from beneath the main minifilament eruption; it dominates the 94 Å emission. Overlaid magnetograms in (c) and (f) are as in Fig. 2, at times of 23:58 UT in both panels.

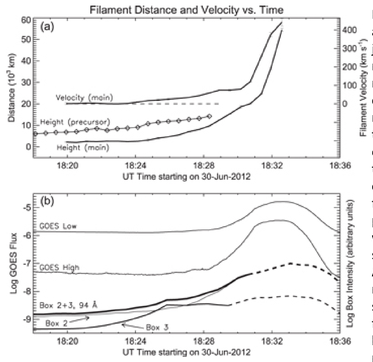

Fig. 6. Trajectories (projected against the disk) as functions of time of the minifilaments of the jet of Fig. 5, and the velocity curve of the main minifilament. Error bars on the main minifilament and velocity are 1σ standard deviations from three independent measurements. The precursor-minifilament trajectory is from a single measurement, but we expect the uncertainties to be similar to those of the main minifilament. In (b), the bottom two curves are AIA 94 Å -channel summed fluxes from the boxed regions in Fig. 3(d). The dashed portions of the curves in (b) are from times when intensity values are not reliable due to saturation or scattering.
A key point is that the jet-producing minifilament's eruption-onset trajectory evolves similarly to the way that of large-scale eruting fialments evolve; e.g. with a slow-rise followed by faster rise, and with acceleration occurring prior to peak in flare brightening.

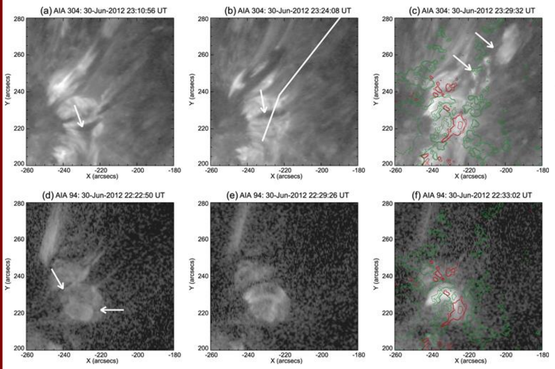

Fig. 7. As in Fig. 5, but for a jet of ~23:30 UT. This event was too weak to produce a detectable GOES soft X-ray signature, and hence is not listed in Table 1. Despite its relative weakness, the jet still resulted from eruption of a minifilament (or multiple minifilament segments). This type of relatively-weak eruption appears to have been common in this active region.

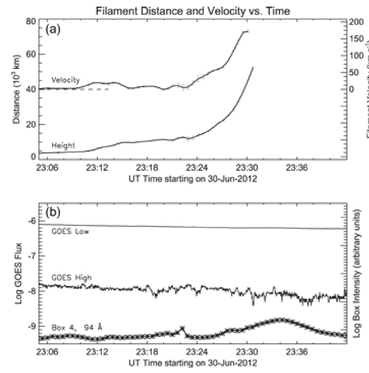

Fig. 8. As in Fig. 6, but for the jet of Fig. 7. As with the event of Figs. 5 and 6, this event's onset has similarities to that of large-scale eruptions, with fast-rise acceleration occurring prior to peak in flare intensity. This supports the suggestion that the same mechanism is operating in both large-scale eruptions and in solar jets.

Main Points and Conclusions:

- Several of our active region jets, including Table 1 events 4 and 10 and the relatively-weak jet of Figs. 7 and 8, result from eruptions of miniature filaments, as in the Fig. 1 schematic. That is, they behave like the polar coronal hole jets of Sterling et al. (2015), and thus they are scaled-down versions of large-scale filament eruptions.
- These minifilaments erupt from magnetic neutral lines (blue and brown arrows of Fig. 2f, for the events discussed here), and the JBP corresponds to a miniature flare.
- For several other strong jets occurring around the red and green arrows of Fig. 2f however, we could *not* confirm whether the jets originated from minifilaments. Although their subsequent evolution was consistent with a minifilament origin, the minifilaments were not clearly seen. We speculate that the minifilaments existed, but were quickly "eaten away" by external reconnection. Further study of such strong (i.e., where the jet spires show relatively strong emission in hot-EUV channels and in X-rays) active region jets is required.
- For many of the jets, magnetic cancelation was clearly occurring at the neutral lines from where the jet-producing minifilament eruptions originated. But emerging flux was also present in these regions, and in some cases it could have played a role in triggering the minifilament eruptions.